

Study of fusion in ${}^6,7\text{Li}+{}^{197}\text{Au}$ at near barrier energies

Shital Thakur¹, Vivek Singh², C.S. Palshetkar³, Vandana Nanal^{1,a}, V.V. Parkar^{1,b}, R.G. Pillay¹, A. Shrivastava³, P.C. Rout³, K. Ramachandran³, and A. Chatterjee³

¹ Department of Nuclear and Atomic Physics, Tata Institute of Fundamental Research, Mumbai - 400005, INDIA

² India based Neutrino Observatory, Tata Institute of Fundamental Research, Mumbai - 400005, INDIA

³ Nuclear Physics Division, Bhabha Atomic Research Centre, Mumbai - 400085, INDIA

Abstract. Excitation functions are measured for complete fusion and transfer reactions of ${}^6\text{Li}$ and ${}^7\text{Li}$ with ${}^{197}\text{Au}$ at energies around the Coulomb barrier. Coupled channel calculations including the couplings to both target and projectile excited states have been performed and are found to explain the data at energies below the barrier. At above barrier energies the complete fusion cross sections are found to be suppressed compared to the coupled channel calculations for both the systems. A systematic comparison of fusion cross-section for halo nuclei ${}^6,8\text{He}$ and weakly bound stable nuclei ${}^6,7\text{Li}$ on ${}^{197}\text{Au}$ target is also presented. Large neutron transfer cross-sections are observed for ${}^6,7\text{Li}$ as compared to tightly bound projectiles ${}^{12}\text{C}, {}^{16}\text{O}$.

1 Introduction

The dynamics of complete fusion and breakup reactions induced by weakly bound stable nuclei have been extensively studied in recent years [1]. The weakly bound stable nuclei like ${}^6,7\text{Li}$, ${}^9\text{Be}$, with a well defined cluster structure and small separation energies have a large breakup probability. It is now well established that couplings to internal degrees of freedom of target/projectile nuclei have a strong influence on fusion process at near and sub-barrier energies. Theoretical models involving dynamic interactions such as coupling to low lying rotational states (arising due to nuclear deformation) and/or vibrational states (due to surface modes) of colliding nuclei, predict the fusion cross section enhancement at sub-barrier energies over the 1D barrier penetration model [2]. The experimental study of reactions with weakly bound nuclei and heavy mass targets have shown an enhancement in the cross section at sub-barrier energies and suppression at above barrier energies compared to 1D barrier penetration model. Also, in case of reactions with radioactive ion beams it has been observed that coupling to transfer channel results in large enhancement of fusion probability [3]. Recent results with ${}^8\text{He}$ on ${}^{197}\text{Au}$ target, indicate that the sub-barrier total reaction cross section is completely dominated by direct reactions, in the form of 1n and 2n stripping [4]. Further, the σ_{2n}/σ_{1n} ratio can provide information on structural correlations [5]. A simultaneous measurement of direct and compound nuclear processes with weakly bound nuclei can therefore be used to study the influence of direct reactions on fusion process. In this paper, we present the excitation function

measurement for complete fusion and transfer reaction in ${}^6,7\text{Li} + {}^{197}\text{Au}$ over an energy range of $0.6 \leq E/V_b \leq 1.5$. A systematic comparison of fusion and transfer processes of weakly bound stable nuclei with halo and tightly bound projectiles is also presented.

2 Experimental Details

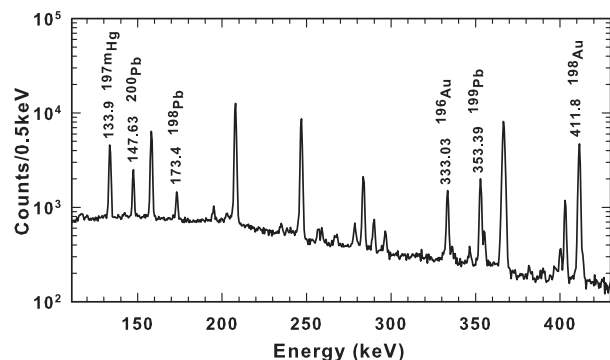
Self supporting, rolled target foils of ${}^{197}\text{Au}$ (~ 1.5 - 1.65 mg/cm² thick) were irradiated with ${}^6,7\text{Li}$ beams of energies 23-44 MeV ($I \sim 10$ -20 pA) from the Pelletron Linac facility, Mumbai. Aluminum catcher foils of thickness ~ 3 mg/cm² were mounted behind the target to capture all reaction products. For optimal utilization of the beam time, cascaded targets with aluminum degrader foils were used in some cases. The beam current was recorded at regular preset intervals (10 to 30 s) during irradiation. Products originating from complete fusion and transfer reactions are predominantly beta active with long half-lives (12 min to 3 days) and were measured by off-line gamma counting. The irradiated target along with the catcher foil was mounted at a distance of ~ 10 cm from an efficiency calibrated HPGe detector. For data collection at sub-barrier energies, the detector was housed inside a low background setup consisting of graded shielding of thin Ni+Cd foils and 5cm thick lead and the target was mounted in a close geometry. Data was recorded using a CAMAC based acquisition system LAMPS. Table 1 lists half-lives of reaction products together with their characteristic γ -rays and branching ratios. Figure 1 shows a typical off-line γ -ray spectrum for ${}^6\text{Li} + {}^{197}\text{Au}$ at $E_{\text{lab}} = 40\text{MeV}$. Half-lives of various γ -rays were followed for unambiguous identification of the residues. The cross sections of various channels were extracted from observed γ -ray yields. For many of the decay

^a e-mail: nanal@tiffr.res.in

^b Present address: Departamento de Fisica Aplicada, Universidad de Huelva, E-21071 Huelva, Spain

Table 1. Reaction products with half-lives ($T_{1/2}$), characteristic γ -rays and relative intensities I_γ (%) [6].

| | Nuclide | $T_{1/2}$ | E_γ (keV) | I_γ (%) |
|---------------------|--------------------|-------------------|------------------|----------------|
| Evaporation residue | ^{201}Pb | 9.33 h | 331.15 | 77 |
| | | | 945.96 | 7.2 |
| | ^{200}Pb | 21.5 h | 147.63 | 38.2 |
| | | | 257.19 | 4.52 |
| | ^{199}Pb | 90 m | 353.39 | 9.5 |
| | | | 720.24 | 6.5 |
| | | | 1135.04 | 7.8 |
| ^{199m}Pb | 12.2 m | 424.1 | 10 | |
| | ^{198}Pb | 2.4 h | 173.4 | 18.2 |
| | | 865.3 | 6.0 | |
| Transfer | ^{199}Au | 3.139 d | 158.38 | 40.0 |
| | | | 208.20 | 8.72 |
| | ^{198}Au | 2.695 d | 411.8 | 95.58 |
| | | ^{196}Au | 6.183 d | 333.03 |
| | | | 355.73 | 87 |
| | ^{197m}Hg | 23.8 h | 133.98 | 33.5 |

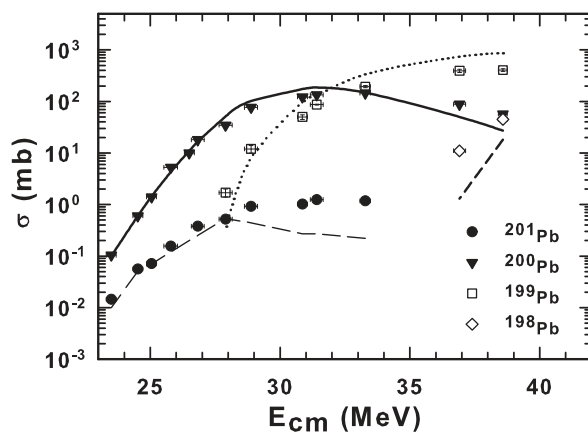
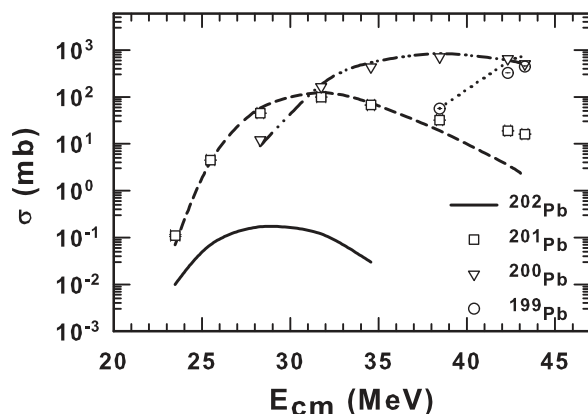
**Fig. 1.** A typical off-line γ -ray spectrum measured in $^6\text{Li} + ^{197}\text{Au}$ reaction at $E_{\text{lab}} = 40\text{MeV}$, where lines of interest have been labelled.

products, more than one γ -ray were observed and extracted cross sections from different γ -rays were consistent within a few %.

3 Data Analysis and Results

3.1 Complete Fusion cross sections

Figures 2 and 3 show the measured excitation function for residues arising from the compound nuclear fusion in reaction $^6\text{Li} + ^{197}\text{Au}$ ($V_b=29.3\text{ MeV}$) and $^7\text{Li} + ^{197}\text{Au}$ ($V_b=29\text{ MeV}$), respectively. In the latter case, the evaporation residue ^{202}Pb (2n channel), being stable could not be detected in off-line counting. However, the contribution from this decay channel is expected to be negligible in the energy region of interest. The statistical model calculations (lines) performed with PACE2 [7] employing Ignatyuk level density prescription with level density param-

**Fig. 2.** Measured excitation function for evaporation residues from compound nuclear decay in $^6\text{Li} + ^{197}\text{Au}$ (symbols) reaction together with statistical model calculations (lines) using PACE2**Fig. 3.** Same as Fig. 2 for $^7\text{Li} + ^{197}\text{Au}$

eter $A/9\text{ MeV}^{-1}$ are in good agreement with data (symbols). The compound nuclear angular momentum distribution obtained from coupled channel code CCFULL[8] was used as input for these calculations. The total fusion cross sections were obtained from the sum of partial residue cross sections. The coupled channel calculations were performed using code CCFULL[8], including the coupling to the first excited state in the projectile (i.e. to the unbound 3^+ , 2.186 MeV state of ^6Li , and to the bound $1/2^-$, 0.478 MeV of ^7Li). In addition, a coupling to the target inelastic state with deformation parameter $\beta_2 = 0.1$ has also been included. The results thus obtained are shown in figure 4. The 1D barrier penetration model calculations for ^6Li are also shown for comparison. It is clearly seen that the CCFULL calculations are in excellent agreement with experimental data at energies below the barrier for both $^6,7\text{Li}$, but at above barrier energies measured cross-sections are lower than the CCFULL prediction. It should be pointed out that the suppression of measured cross-sections at higher energies is much more significant in case of ^6Li than in ^7Li .

Scaled cross sections are obtained using procedure described in ref. [9] taking into account experimental values

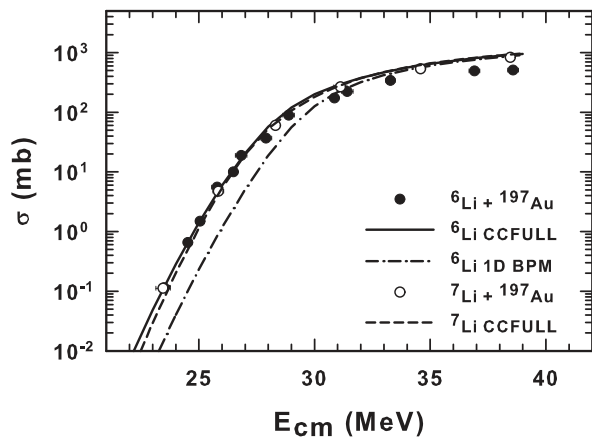


Fig. 4. Experimental complete fusion cross sections for ${}^6,7\text{Li} + {}^{197}\text{Au}$ together with CCFULL calculations for ${}^6\text{Li}$ (solid line) and ${}^7\text{Li}$ (dashed line). The 1D BPM prediction (dot-dashed line) for ${}^6\text{Li}$ is also shown for comparison

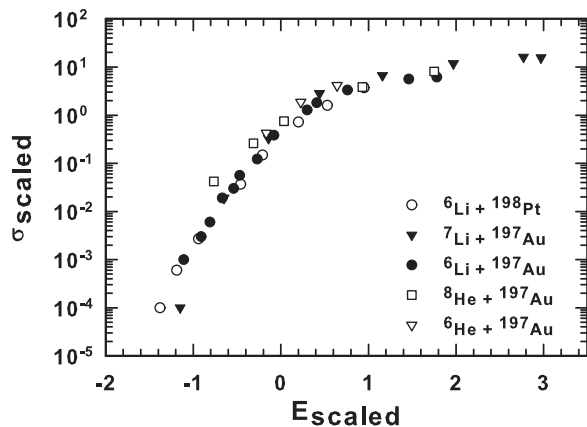


Fig. 5. Comparison of reduced fusion cross sections (adopted from [9]) for ${}^6\text{Li} + {}^{198}\text{Pt}$ [11], ${}^6\text{He} + {}^{197}\text{Au}$ [10], ${}^8\text{He} + {}^{197}\text{Au}$ [4] together with present data ${}^6,7\text{Li} + {}^{197}\text{Au}$.

of the fusion cross section and height, radius and curvature of the barrier. Figure 5 shows a systematic comparison of the present data with ${}^6,8\text{He}$ on ${}^{197}\text{Au}$ from ref. [4,10]. The ${}^6\text{Li} + {}^{198}\text{Pt}$ [11] is also shown in the same figure. The scaled cross-sections for ${}^6\text{Li}$ on ${}^{197}\text{Au}$ and ${}^{198}\text{Pt}$ are very similar, indicating no significant target dependence. Similar results have been reported in [12] and [13] showing no target dependence. A large enhancement of the scaled fusion cross section for halo nucleus ${}^8\text{He}$ as compared to the weakly bound nuclei is clearly seen at sub-barrier energies.

3.2 Transfer cross sections

In case of weakly bound projectiles like ${}^6,7\text{Li}$ the contribution from transfer and breakup processes is expected to be significant. The d/t transfer leads to Hg isotopes which are stable and could not be measured in the present experiment. However, the isomeric state ${}^{197m}\text{Hg}$ resulting from

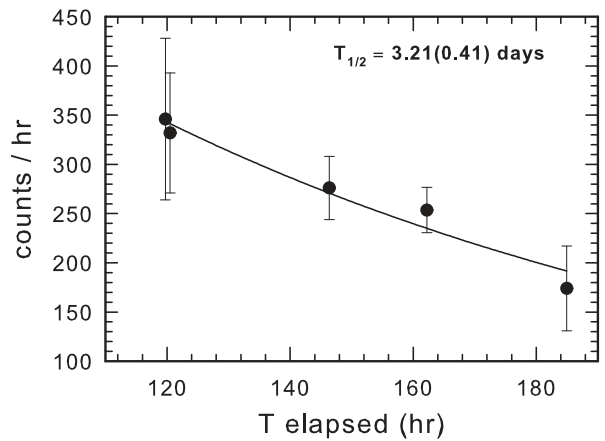


Fig. 6. Decay curve for ${}^{199}\text{Au}$ with $E_\gamma=158.4$ keV in ${}^7\text{Li} + {}^{197}\text{Au}$ reaction at $E_{\text{lab}}=33\text{MeV}$

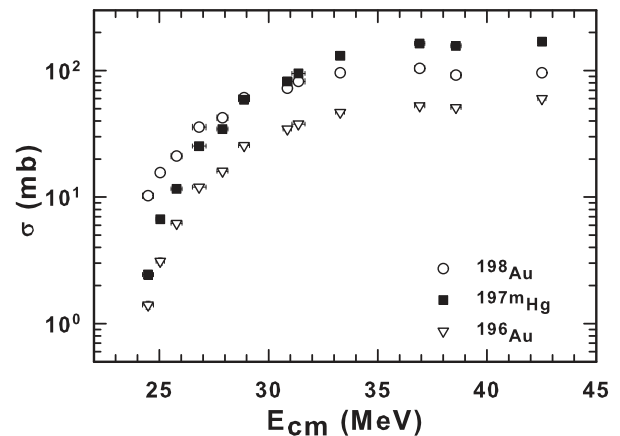


Fig. 7. Measured excitation function for transfer products in ${}^6\text{Li} + {}^{197}\text{Au}$ reaction

(d,2n) is observed in ${}^6\text{Li}$ induced reaction and its cross section has been measured. In ${}^6\text{Li}$ induced reaction, 1n pickup (${}^{196}\text{Au}$) and 1n stripping (${}^{198}\text{Au}$) channels are seen while in case of ${}^7\text{Li}$, 1n and 2n stripping (${}^{198,199}\text{Au}$) channels are observed. It should be mentioned that care has to be taken while extracting the 2n stripping cross-sections in the present case. The daughter nucleus ${}^{199}\text{Hg}$ is populated via β decay of ${}^{199}\text{Au}$ (2n stripping, 3.139 days) and via EC of ${}^{199}\text{Tl}$ (7.42 hrs) which is a granddaughter of 5n evaporation channel (${}^{199}\text{Pb}$). Therefore for measurement of 2n stripping cross-section, data collection was done 60 hours after irradiation (~ 8 half-lives of ${}^{199}\text{Tl}$). Figure 6 shows a typical decay plot of ${}^{199}\text{Au}$ at $E_{\text{lab}} = 33\text{MeV}$, where the measured half-life value is in excellent agreement with reference value listed in Table 1 indicating that the contribution from the ${}^{199}\text{Tl}$ nucleus is negligible.

The measured excitation functions for transfer products in ${}^6,7\text{Li} + {}^{197}\text{Au}$ reactions are shown in figures 7 and 8. It should be mentioned that at very low energy, σ_{1n} is larger than σ_{fusion} . Similar energy dependence has been reported in ${}^6\text{He} + {}^{197}\text{Au}$ reaction for production of ${}^{198}\text{Au}$ [10], while

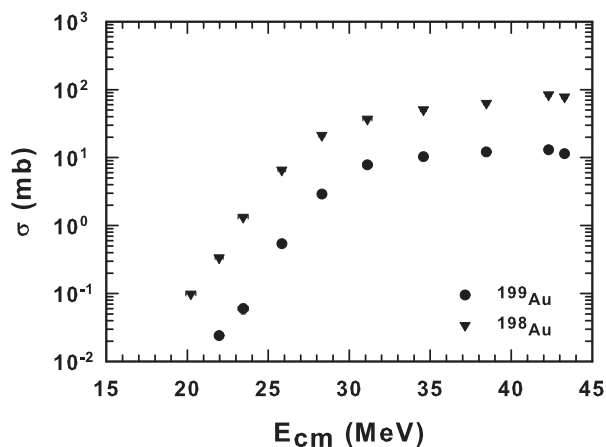


Fig. 8. Same as Fig. 7 for ${}^7\text{Li} + {}^{197}\text{Au}$ reaction

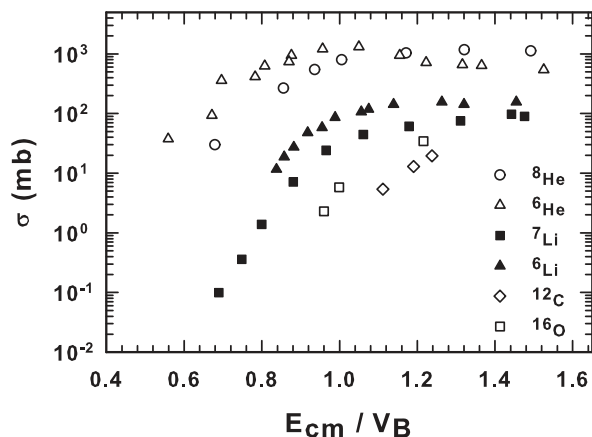


Fig. 9. A systematic comparison of transfer cross sections for halo nuclei [4, 10], weakly bound nuclei (present data) and tightly bound nuclei [14] on ${}^{197}\text{Au}$ target

the absolute magnitude of σ_{1n} is considerably large (>1 barn). A systematic comparison of transfer cross sections with ${}^6,8\text{He}$ (halo nuclei), ${}^6,7\text{Li}$ (weakly bound nuclei) and ${}^{12}\text{C}$, ${}^{16}\text{O}$ (tightly bound stable nuclei) is shown in figure 9. In case of ${}^6,8\text{He}$, large Q value of $2n$ transfer leads to population of particle un-bound states in ${}^{199}\text{Au}$ and therefore is followed by neutron evaporation(s) [4, 10]. Thus, the observed ${}^{198}\text{Au}$ cross-section contains contribution both from $1n$ and $2n$ transfer. Hence, in the figure total transfer cross sections, i.e., $1n$ stripping + $1n$ pickup for ${}^6\text{Li}$ and $1n + 2n$ stripping for ${}^7\text{Li}$ are plotted. It can be seen that at sub-barrier energies, large n -transfer cross-sections are observed for both ${}^6,7\text{Li}$ compared to stable nuclei, while those for halo nuclei are even larger (as expected).

4 Summary and Conclusion

In summary, the excitation function for complete fusion in the ${}^6,7\text{Li} + {}^{197}\text{Au}$ systems has been measured at ener-

gies around the Coulomb barrier. The fusion cross sections show enhancement below the barrier as compared to 1D BPM. The Coupled channel calculations incorporating couplings to the inelastic excitation of target and projectiles are able to explain the data at sub-barrier energies. The measured fusion cross sections above the barrier are suppressed as compared to the CCFULL calculation, while suppression is more significant in case of ${}^6\text{Li}$ than in ${}^7\text{Li}$. A comparison of scaled fusion cross-sections for ${}^6,8\text{He}$ and ${}^6,7\text{Li}$ has also been presented. Large neutron transfer cross-sections are observed for ${}^6,7\text{Li}$ as compared to tightly bound projectiles ${}^{12}\text{C}$, ${}^{16}\text{O}$.

In both ${}^6,7\text{Li}$ induced reactions the breakup channel is very important. In the present off-line experiment, d/t capture leading to stable Hg isotopes and α capture leading to Tl isotopes (which are also produced by decay of fusion residues- Pb isotopes) could not be extracted. The measurement of breakup fusion products by online gamma spectroscopy is planned and will help in understanding the effect of breakup in reactions with weakly bound nuclei.

Authors would like to thank Ms. D. Thapa for target preparation, Mr. M.S. Pose for help during the experiment and the accelerator staff for smooth operation.

References

1. P.R.S. Gomes et al., Nucl. Phys. A **734**, (2004) 233
2. L.F. Canto et al., Physics Reports **424**, (2006) 1
3. N. Keeley et al., Prog. Part. Nucl. Phys. **59**, (2007) 579
4. A. Lemasson et al., Phys. Rev. Lett. **103**, (2009) 232701
5. A. Chatterjee et al., Phys. Rev. Lett. **101**, (2008) 032701
6. <http://www.nndc.bnl.gov/nudat2/>
7. A. Gavron, Phys. Rev. C **21**, (1980) 230
8. K. Hagino et al., Computer Physics Communications **123**, (1999) 143
9. L.F. Canto et al., J. Phys. G **36**, (2009) 015109
10. Yu. E. Penionzhkevich et al., Eur. Phys. J. A **31**, (2007) 185
11. A. Shrivastava et al., Phys. Rev. Lett. **103**, (2009) 232702
12. M. Dasgupta et al., Phys. Rev. C **70**, (2004) 024606
13. P.K. Rath et al., Phys. Rev. C. **79**, (2009) 051601
14. A. Yokoyama et al., Z. Phys. A **332**, (1989) 61